HHS Public Access

Author manuscript

Virology. Author manuscript; available in PMC 2017 January 01.

Published in final edited form as:

Virology. 2016 January ; 487: 273–284. doi:10.1016/j.virol.2015.10.024.

Phosphorylation of mouse SAMHD1 regulates its restriction of human immunodeficiency virus type 1 infection, but not murine leukemia virus infection

Feifei Wang[1], **Corine St. Gelais**[1], **Suresh de Silva**[1,*], **Hong Zhang**[2], **Yu Geng**[2], **Caitlin Shepard**[3], **Baek Kim**[3], **Jacob S. Yount**[4,5], and **Li Wu**[1,4,6,§]

[1] Center for Retrovirus Research, Department of Veterinary Biosciences, The Ohio State University, 1900 Coffey Road, Columbus, Ohio

[2] ProSci, Inc., 12170 Flint Place, Poway, California

[3] Department of Pediatrics, Center for Drug Discovery, Emory University School of Medicine, 1760 Haygood Drive, Atlanta, Georgia

[4] Center for Microbial Interface Biology, The Ohio State University, 1900 Coffey Road, Columbus, Ohio

[5] Department of Microbial Infection and Immunity, The Ohio State University, 1900 Coffey Road, Columbus, Ohio

[6] Comprehensive Cancer Center, The Ohio State University, 1900 Coffey Road, Columbus, Ohio

Abstract

Human SAMHD1 (hSAMHD1) restricts HIV-1 infection in non-dividing cells by depleting intracellular dNTPs to limit viral reverse transcription. Phosphorylation of hSAMHD1 at threonine (T) 592 by cyclin-dependent kinase (CDK) 1 and CDK2 negatively regulates HIV-1 restriction. Mouse SAMHD1 (mSAMHD1) restricts HIV-1 infection in non-dividing cells, but whether its phosphorylation regulates retroviral restriction is unknown. Here we identified six phospho-sites of mSAMHD1, including T634 that is homologous to T592 of hSAMHD1 and phosphorylated by CDK1 and CDK2. We found that wild-type (WT) mSAMHD1 and a phospho-ablative mutant, but not a phospho-mimetic mutant, restricted HIV-1 infection in differentiated U937 cells. Murine leukemia virus (MLV) infection of dividing NIH3T3 cells was modestly restricted by mSAMHD1 WT and phospho-mutants, but not by a dNTPase-defective mutant. Our results suggest that phosphorylation of mSAMHD1 at T634 by CDK1/2 negatively regulates its HIV-1 restriction in differentiated cells, but does not affect its MLV restriction in dividing cells.

§ Corresponding author. Li Wu, Center for Retrovirus Research, The Ohio State University, 1900 Coffey Road, Columbus, Ohio 43210, USA. wu.840@osu.edu Phone: 614-292-5408.

*Current address: Heat Biologics, Inc., 801 Capitola Drive, Durham, NC 27713.

Keywords

Mouse and human SAMHD1; Phosphorylation; HIV-1; MLV; Infection; Restriction

Introduction

Sterile α motif (SAM) and HD domain containing protein 1 (SAMHD1) is a deoxynucleotide triphosphohydrolase (dNTPase) (Goldstone et al., 2011; Powell et al., 2011) and functions as an HIV-1 restriction factor in non-dividing myeloid cells and resting $CD4^+$ T cells (Baldauf et al., 2012; Hrecka et al., 2011; Laguette et al., 2011a). Human SAMHD1 (hSAMHD1) inhibits infection of a wide range of retroviruses including HIV-1 and murine leukemia virus (MLV) (Gramberg et al., 2013), and DNA viruses, such as herpes simplex virus type 1 in human macrophages (Kim et al., 2013). The dNTPase activity of SAMHD1 enables it to decrease intracellular dNTPs to below the levels required for retroviral replication (Lahouassa et al., 2012), a general mechanism by which hSAMHD1 impedes viral infection (Wu, 2013).

SAMHD1 is a conserved protein in humans and mice (Yang et al., 2014). The mouse SAMHD1 gene contains two start codons, and it is possible that both start codons are used for translation in vivo. Alternative splicing of the mSAMHD1 pre-mRNA results in two isoforms of the protein (isoform 1 and 2), which share 72% and 74% protein sequence identities with hSAMHD1. Both mSAMHD1 isoforms possess dNTPase activity (Lahouassa et al., 2012; Powell et al., 2011; Zhang et al., 2014), and isoform 1 mRNA is more abundantly expressed than isoform 2 mRNA in various mouse tissues (Zhang et al., 2014). Compared to hSAMHD1 wild-type (WT) or phospho-ablative mutants, phospho-mimetic mutants at residue T592 lose their HIV-1 restriction phenotype in non-dividing cells (Cribier et al., 2013; Pauls et al., 2014; St Gelais et al., 2014; Welbourn et al., 2013; White et al., 2013b). It has been proposed that T592 phosphorylation of hSAMHD1 negatively regulates its RNase activity in cells and may affect HIV-1 restriction (Ryoo et al., 2014). These studies suggest that T592 phosphorylation of hSAMHD1 plays a role in regulating its HIV-1 restriction function. However, there is no evidence linking the phosphorylation of mSAMHD1 to its retroviral restriction phenotype. It is also unknown whether mSAMHD1 and hSAMHD1 restrict HIV-1 and MLV through the same mechanism.

Here, we aim to elucidate the contribution of mSAMHD1 phosphorylation to its retroviral restriction function in cells. We identified that T634 is a phosphosite of mSAMHD1 isoform 1 (refer to as mSAMHD1 unless isoform 2 is indicated) and demonstrated that CDK1 and CDK2 phosphorylate mSAMHD1 at T634 in dividing cells. We examined the effect of T634 phosphorylation on mSAMHD1-mediated restriction of HIV-1 or MLV in human and mouse cell lines stably expressing mSAMHD1 WT, phospho-ablative, phospho-mimetic or dNTPase-defective mutants. We found that T634 phosphorylation of mSAMHD1 regulates its HIV-1 restriction in differentiated human U937 cells. In dividing mouse NIH3T3 cells, overexpression of mSAMHD1 or hSAMHD1 modestly restricts MLV infection, which is independent of T634 phosphorylation of mSAMHD1. Our results demonstrate that phosphorylation of mSAMHD1 modulates its restriction of HIV-1 infection in non-dividing

cells, but not MLV infection in dividing cells, suggesting different mechanisms of regulating retroviral restriction by hSAMHD1 and mSAMHD1.

Results

Identification of phosphorylation sites of mSAMHD1 protein

Mouse SAMHD1 was identified as a phosphoprotein in previous large-scale analyses of phosphorylated proteins (Sweet et al., 2009; Villen et al., 2007; Zanivan et al., 2008). The C-terminal protein sequences of human and mouse SAMHD1 are highly conserved (Yang et al., 2014), and contain the residue T592 in hSAMHD1 and a predicted phosphosite at position T634 in mSAMHD1 isoform 1 with the first start codon aligning with the start codon of hSAMHD1 (Cribier et al., 2013; Villen et al., 2007). In non-dividing cells, WT hSAMHD1 and a phospho-ablative mutant (T592A) restrict HIV-1 infection, while phospho-mimetic mutants of hSAMHD1 lose HIV-1 restriction (Cribier et al., 2013; Welbourn et al., 2013; White et al., 2013b), suggesting that phosphorylation negatively affects the HIV-1 restriction function of hSAMHD1. We thus questioned whether phosphorylation at T634 could be a negative regulatory mechanism for mSAMHD1-mediated restriction of retroviral infection. Given that mSAMHD1 isoform 1 is more abundantly expressed compared to isoform 2, in multiple tissues (Zhang et al., 2014), we focused our study on mSAMHD1 isoform 1.

To identify phosphosites of mSAMHD1, tandem mass spectrometry (MS/MS) was performed with phosphorylation modification analysis after immunoprecipitation of full-length mSAMHD1 isoform 1 (St Gelais et al., 2014). A total of 678 peptides were assigned to mSAMHD1 providing 72% coverage of the protein. Six phosphorylated residues were identified including threonines 52, 56, 310, and 634, and serines 55 and 140 (Table 1). Figure 1 shows a representative MS/MS spectrum for the peptide that allowed identification of T634 phosphorylation of mSAMHD1 isoform 1. There were 36 peptides identified covering this region, of which 17 corresponded to phosphorylated T634, providing strong confidence in phospho-modification of this residue. Interestingly, based on sequence alignment of mSAMHD1 and hSAMHD1 (Fig. 2A), T634 is homologous to the known T592 phosphosite of hSAMHD1 that negatively regulates hSAMHD1-mediated HIV-1 restriction (Cribier et al., 2013; St Gelais et al., 2014; Welbourn et al., 2013; White et al., 2013b).

To confirm the phosphorylation status of mSAMHD1 isoform 1 at T634 in cells, we generated a phospho-specific SAMHD1 antibody, whose epitope targets the consensus C-terminal sequences of hSAMHD1 and mSAMHD1 encompassing the phospho-sites T592 and T634. Thus, the antibody can specifically detect T592 phosphorylated hSAMHD1 and T634 phosphorylated mSAMHD1. We generated two mSAMHD1 isoform 1 mutants substituting threonine with a phospho-ablative alanine residue (T634A) or phospho-mimetic aspartic acid residue (T634D). Transient overexpression of mSAMHD1 WT, T634A or T634D in HEK293T cells was detected by immunoblotting. Total hSAMHD1 was detected at 72 kDa, while mSAMHD1 WT and mutants were detected at 76 kDa, as expected (Fig. 2B). Phosphorylation of hSAMHD1 at T592 and mSAMHD1 isoform 1 at T634 was detected using the specific phospho-SAMHD1 antibody. As expected, phospho-ablative and

phospho-mimetic mutants of mSAMHD1 isoform 1 had no detectable signal when using the specific phospho-SAMHD1 antibody (Fig. 2B). Moreover, to test whether the endogenous mSAMHD1 is also phosphorylated, we performed immunoblotting with lysates from mouse fibroblast NIH3T3 cells and mouse embryonic fibroblasts (MEFs). Specific SAMHD1 bands were detected in MEFs using a SAMHD1 antibody and a phospho-SAMHD1 antibody (Fig. 2C), suggesting that endogenous mSAMHD1 is also phosphorylated at T634 in primary mouse fibroblasts. In contrast, a very low level of endogenous mSAMHD1, but not the T634 phosphorylated protein, was detected in NIH3T3 cells (Fig. 2C), which might be due to detection limit of the phospho-SAMHD1 antibody.

CDK1 and CDK2 contribute to T634 phosphorylation of mSAMHD1 in HEK293T cells

The CDK1/CDK2 and cyclin A2 complex phosphorylates hSAMHD1 at position T592 in dividing cells (Cribier et al., 2013; Pauls et al., 2014; St Gelais et al., 2014; White et al., 2013b). Our previous results showed that both hSAMHD1 and mSAMHD1 interact with CDK1 and CDK2 in HEK293T cells (St Gelais et al., 2014). Similar to T592 in hSAMHD1, T634 of mSAMHD1 is located within a predicted CDK-binding motif, TPXK (Cribier et al., 2013) (Fig. 2A); therefore, it is possible that CDK1 and CDK2 could be responsible for the phosphorylation of mSAMHD1 at T634.

To determine whether CDK1 and CDK2 contribute to phosphorylation of mSAMHD1 at T634, we first inhibited the kinase activities of CDK1 and CDK2 using specific inhibitors. HEK293T cells were pretreated with specific inhibitors for 6 hr, and transfected to transiently express mSAMHD1 WT. Cell lysates were collected 24 h post-transfection and used for immunoblotting to determine the levels of total and phospho-SAMHD1. To evaluate changes in the level of phospho-mSAMHD1, the relative level of phospho/total mSAMHD1 was calculated after GAPDH normalization based on densitometry analysis of these protein bands. Compared to control cells treated with DMSO, individual and combined treatments with inhibitors to CDK1 and CDK2 reduced the relative levels of phospho-mSAMHD1 by 62% ($P < 0.01$), 34% ($P < 0.05$), and 66% ($P < 0.01$), respectively (Fig. 3A and 3B). These results suggest that both CDK1 and CDK2 phosphorylate mSAMHD1 at T634 in dividing human cells.

To exclude the potential off-target effect of using specific inhibitors to CDK1 and CDK2, we also used well-characterized dominant negative (DN) mutants of CDK1 and CDK2 (van den Heuvel and Harlow, 1993) to abolish their kinase activities. HEK293T cells were transiently transfected to express mSAMHD1 WT together with WT or dominant negative (DN) mutants of CDK1 or CDK2. Overexpression of hemagglutinin (HA)-tagged CDK1 or CDK2 was confirmed by immunoblotting. The levels of total and phospho-mSAMHD1 were confirmed and quantified by densitometry analysis of these protein bands (Fig. 3C). Summarized results of three independent experiments are presented in Fig. 3D. We found that the level of phospho-mSAMHD1 was reduced by 25% in cells overexpressing CDK1 DN compared to CDK1 WT. Interestingly, when we compared cells overexpressing CDK2 DN to CDK2 WT, the CDK2 DN exhibited a much stronger effect and the level of phospho-mSAMHD1 was reduced by 84% ($P<0.05$) (Fig. 3D). These results suggest that both CDK1

and CDK2 contribute to T634 phosphorylation of mSAMHD1 in dividing cells and that CDK2 likely plays a more important role than CDK1.

To confirm that endogenous CDK1 and CDK2 contribute to phosphorylate mSAMHD1 at T634 in HEK293T cells, we used specific siRNA mediated knockdown (KD) of CDK1 and CDK2 as an alternative method. After two rounds of siRNA transfections, we effectively reduced the expression of CDK1 by approximately 95% and CDK2 by 73% in HEK293T cells (Fig. 3E). Compared to control cells transfected with non-specific siRNA, knockdown of CDK1 and CDK2 decreased the relative levels of phospho-mSAMHD1 by 54% and 60%, respectively (Fig. 3F). When CDK1 and CDK2 were knocked down together, the relative level of phospho-mSAMHD1 was reduced by 73% ($P < 0.05$) (Fig. 3F), suggesting a synergistic or additive effect of the double KD. Using three different approaches, we further confirmed that CDK1 and CDK2 contribute to phosphorylation of mSAMHD1 at T634.

Endogenous CDK1 and CDK2 phosphorylate mSAMHD1 at T634 in mouse fibroblast cells

Because CDK1 and CDK2 are highly conserved in human and mice (Malumbres and Barbacid, 2005) and share 97% and 85% amino acid identity, respectively, it is expected that mSAMHD1 could be phosphorylated by endogenous mouse CDK1 and CDK2. To validate whether endogenous CDK1 and CDK2 phosphorylate mSAMHD1 at T634 in dividing mouse cells, murine fibroblast NIH3T3 cells lacking a high level of endogenous mSAMHD1 were transduced to stably express mSAMHD1. These transduced NIH3T3 cells were treated with inhibitors specific to CDK1 or CDK2. To avoid cytotoxicity of the inhibitors, cell viability was tested in the presence of the inhibitors at different concentrations (0.1-1.0 μM). Based on the titration results and our previous published results (St Gelais et al., 2014), cells were treated with 0.1 or 0.5 μM of the inhibitors. Cell lysates were collected 24 h after treatment and level of total and phospho-mSAMHD1 was confirmed by immunoblotting (Fig. 4A). Individual and combined treatments using 0.1 μM CDK1 and CDK2 inhibitors reduced the relative levels of phospho-mSAMHD1 by approximately 2-fold compared to control cells treated with DMSO (Fig. 4A and 4B). Utilizing a higher concentration of 0.5 μM, individually or in combination, reduced the relative levels of phospho-mSAMHD1 by 45% ($P > 0.05$), 78% ($P < 0.05$), and 83% ($P < 0.05$) compared to DMSO treatment (Fig. 4A and 4B). These results confirm that endogenous CDK1 and CDK2 contribute to T634 phosphorylation of mSAMHD1 in mouse dividing cells.

The effect of T634 phosphorylation of mSAMHD1 on restriction of HIV-1 infection in differentiated U937 cells

Previous studies reported that mSAMHD1 restricts HIV-1 infection in non-dividing cells (Hofmann et al., 2012; Lahouassa et al., 2012). Because T634 of mSAMHD1 is a confirmed phosphosite that is homologous to T592 of hSAMHD1, and hSAMHD1-mediated HIV-1 restriction can be negatively regulated by T592 phosphorylation in non-dividing cells (Cribier et al., 2013; Welbourn et al., 2013; White et al., 2013b), it is conceivable that T634 phosphorylation also negatively regulates mSAMHD1-mediated HIV-1 restriction in non-dividing cells. We thus sought to examine the importance of T634 phosphorylation in regulating mSAMHD1-mediated HIV-1 restriction in a non-dividing cell model. Using the lentiviral vectors previous described (Hofmann et al., 2012; St Gelais et al., 2014), we

generated human U937 cell lines that stably express mSAMHD1 isoform 1 WT, the T634 phospho-mutants, or isoform 2 WT that lacks the T634 phosphorylation at the C-terminus (Fig. 5A); hSAMHD1 WT was used as a positive control for HIV-1 restriction (Welbourn et al., 2013; White et al., 2013b). We confirmed comparable expression levels of SAMHD1 WT or mutant in non-dividing U937 cells differentiated with phorbol 12-myristate 13-acetate (PMA) (Fig. 5B).

To investigate the effect of T634 phosphorylation of mSAMHD1 on its HIV-1 restriction, we performed single-cycle HIV-1 infection of U937 cells expressing SAMHD1 WT and mutants after PMA differentiation. HIV-1 infection was measured at 24 h post-infection. We observed HIV-1 restriction in cells expressing WT hSAMHD1, WT mSAMHD1 isoform1 or T634A mutant, and WT mSAMHD1 isoform 2, but not in cells expressing the phospho-mimetic mutants of mSAMHD1 isoform1 (T634D) compared to vector control cells (Fig. 5C). Our data suggest a negative regulation of HIV-1 restriction by T634 phosphorylation of mSAMHD1, which is consistent with the effect of T592 phosphorylation on hSAMHD1-mediated HIV-1 restriction (Cribier et al., 2013; Gramberg et al., 2013; Hofmann et al., 2012; St Gelais et al., 2014; Welbourn et al., 2013; White et al., 2013b).

To verify whether HIV-1 restriction by mSAMHD1 WT or mutants in PMA-differentiated U937 cells was due to a reduced dNTP pool, the intracellular dNTP levels were measured using the single nucleotide incorporation assay (St Gelais et al., 2012). Compared to PMA-differentiated vector control U937 cells, the intracellular dNTP levels in cells expressing mSAMHD1 WT or mutants were reduced 2- to 6-fold ($P < 0.0001$) (Fig. 5C). The dNTP levels were comparable among the cells expressing WT hSAMHD1, WT or mutant mSAMHD1 isoform 1, and WT mSAMHD1 isoform 2 (Fig. 5D), suggesting that T634 phosphorylation of mSAMHD1 does not significantly affect its dNTPase function in cells. Our data are consistent with published results that the dNTPase activity of hSAMHD1 is not regulated by its T592 phosphorylation in non-dividing cells (White et al., 2013b).

MLV infection in NIH3T3 cells is reduced by mSAMHD1 independently of its T634 phosphorylation

Knockdown of mSAMHD1 expression in mouse macrophage-like cells relieves SAMHD1's restriction of MLV infection (Zhang et al., 2014). However, whether T634 phosphorylation of mSAMHD1 regulates MLV infection restriction is unknown. To test the importance of T634 phosphorylation in regulating mSAMHD1-mediated MLV restriction, we generated mouse fibroblast cells lines (NIH3T3) that stably express mSAMHD1 isoform1 WT, T634A or T634D mutant, or mSAMHD1 isoform 2. Human SAMHD1 WT and a phospho-ablative mutant (T592A) were included as controls (St Gelais et al., 2014). Comparable expression levels of SAMHD1 WT and mutants in dividing NIH3T3 cells were confirmed by immunoblotting (Fig. 6A). As expected, phosphorylated hSAMHD1 or mSAMHD1 was only detected in cells expressing WT hSAMHD1 and WT or the HD/AA mutant of mSAMHD1 isoform 1, but not the phospho-mutants or mSAMHD1 isoform 2 using the specific phospho-SAMHD1 antibody (Fig. 6A). Next, NIH3T3 cells stably expressing SAMHD1 WT or mutants were infected with a single-cycle GFP reporter MLV and GFP-positive cells were quantified by flow cytometry at 48 h post-infection. Interestingly, the

percentage of GFP-positive cells was reduced by 8.8~15.8% in cells expressing SAMHD1 WT and phospho-mutants ($P < 0.0001$) compared to that in vector control cells (Fig. 6B). These results suggest that restriction of MLV infection in dividing cells by mSAMHD1 is independent of its T634 phosphorylation.

To discriminate whether mSAMHD1 specifically restricts MLV in NIH3T3 cells, we also tested HIV-1 infection in NIH3T3 cells expressing WT hSAMHD1, mSAMHD1 isoform 1, or mSAMHD1 isoform 2. Cells were infected with HIV-1 GFP/VSV-G reporter virus and GFP-positive cells were quantified by flow cytometry at 48 h post-infection. The HIV-1 infection levels did not differ among cell lines expressing WT hSAMHD1, mSAMHD1 isoform 1, or mSAMHD1 isoform 2, compared to vector control cells (Fig. 6C). Thus, HIV-1 infection was not affected by overexpression of WT hSAMHD1, mSAMHD1 isoform1 or isoform 2 in NIH3T3 cells.

To examine whether SAMHD1 inhibited MLV infection in NIH3T3 cells by depleting cellar dNTPs to limit the completion of viral reverse transcription products, we measured intracellular dNTP levels in NIH3T3 cells stably expressing SAMHD1 WT and mutants. In four independent experiments, we observed that dCTP levels were significantly reduced up to 2-fold in NIH3T3 cells expressing SAMHD1 WT or phospho-mutants compared to vector control cells (Fig. 6D), while all the other dNTPs were not significantly affected by SAMHD1 (data not shown). These data suggest that mSAMHD1 WT or phospho-mutants likely maintain a dNTPase activity, but may not significantly reduce the high levels of dNTPs in dividing NIH3T3 cells. These results are consistent with our previous published data that overexpression of hSAMHD1 in dividing HEK293T cells did not significantly reduce the intracellular dNTP pool (St Gelais et al., 2012).

To assess whether the modest reduction of the dCTP levels by mSAMHD1 is required for its inhibition of MLV infection in dividing NIH3T3 cells, we generated a dNTPase-defective mSAMHD1 mutant H238A/D239A (HD/AA). This mSAMHD1 mutant is homologous to the dNTPase-defective mutant H206A/D207A of hSAMHD1, which does not restrict HIV-1 infection in non-dividing cells (Laguette et al., 2011b; White et al., 2013a). After confirmation of comparable expression levels of mSAMHD1 WT and HD/AA mutant in NIH3T3 cells by immunoblotting (Fig. 6A), cells were infected with a single-cycle GFP reporter MLV. Interesting, mSAMHD1 HD/AA mutant did not restrict MLV infection compared to that in vector control cells (Fig. 6B), suggesting that the dNTPase function of mSAMHD1 is required for its MLV restriction.

MLV restriction by SAMHD1 in NIH3T3 cells is correlated with reduced nuclear import of viral cDNA

To examine the mechanisms of MLV restriction by mSAMHD1, we measured the levels of late reverse transcription products in MLV-infected NIH3T3 cells by quantitative PCR. We first verified GFP-reporter MLV infection and SAMHD1-mediated MLV restriction by measuring GFP-positive cells. Treatment of cells with the reverse transcriptase inhibitor azidothymidine (AZT) was used to inhibit reverse transcription, which caused the percentage of GFP-positive cells to significantly reduce to less than 5%, in vector control and SAMHD1-expressing cell lines (Fig. 7A and 7D). The results from three independent

experiments showed no statistical difference between the levels of MLV late reverse transcription products in cells expressing SAMHD1 WT, phospho-mutants or the dNTPase defective mutant relative to that in vector control cells (Fig. 7B and 7E), suggesting that MLV reverse transcription is not affected by SAMHD1 and its T634 phosphorylation in NIH3T3 cells. As expected, AZT treatment significantly decreased late reverse transcription products by approximately 2.2- to 8-fold in the infected cells ($P < 0.05$) (Fig. 7B and 7E).

To assess whether SAMHD1 expression in NIH3T3 cells affected the MLV life cycle at the stage after reverse transcription, we evaluated the levels of MLV 2-LTR circles in the infected cells, which is a surrogate marker for nuclear import of MLV cDNA (Yamashita and Emerman, 2005). The levels of 2-LTR circles in cells expressing SAMHD1 WT or phospho-mutants were reduced by 35.8~52.4% ($P < 0.01$) compared to that in vector control cells, but were not affected by mSAMHD1 HD/AA mutant (Fig. 7C and 7F), indicating that nuclear import of MLV cDNA is limited by SAMHD1 in NIH3T3 cells. These results suggest that mSAMHD1 and hSAMHD1 can moderately restrict MLV infection in dividing mouse cells by limiting the nuclear import of viral cDNA, independent of phosphorylation of SAMHD1.

Discussion

In this study, we identified and confirmed that T634 of mSAMHD1 is phosphorylated by CDK1 and CDK2 in cells. Our results indicate that restriction of HIV-1 infection by mSAMHD1 in non-dividing cells is regulated through its T634 phosphorylation. In contrast, MLV infection in dividing cells is restricted by mSAMHD1 or hSAMHD1 at the stage of viral cDNA nuclear import, which appears to require dNTPase activity, but is independent of T634 phosphorylation.

In addition to T634, we identified five other phosphosites in mSAMHD1 (Table 1). Whether these additional phosphosites regulate the mSAMHD1-mediated restriction of HIV-1 or MLV infection remain to be investigated. Further analysis of these other phosphosites may help to understand the mechanism by which mSAMHD1 restricts retroviral infection in dividing cells.

We found that both CDK1 and CDK2 contribute to T634 phosphorylation of mSAMHD1, which is in agreement with data that hSAMHD1 T592 is mainly phosphorylated by CDK1 and CDK2 (Cribier et al., 2013; Pauls et al., 2014; St Gelais et al., 2014; White et al., 2013b). The relative importance of CDK1 and CDK2 in phosphorylating mSAMHD1 at T634 residue in dividing cells appears different when we used distinct approaches, including specific inhibitors, DN mutants, and siRNA to CDK1 or CDK2 (Fig. 3). This discrepancy could be due to different efficiencies or effects in inhibiting the activities or expression levels of CDK1 and CDK2 using distinct reagents and methods.

As CDK1 and CDK2 are highly conserved between human and mouse, we also confirmed that endogenous mouse CDK1 and CDK2 contributed to T634 phosphorylation of mSAMHD1. Our data showed that residual phosphorylated hSAMHD1 (T592) and mSAMHD1 (T634) were detectable in PMA-differentiated non-dividing U937 cells,

possibly due to expression of CDK2, which unlike CDK1, is not decreased upon PMA-differentiation (St Gelais et al., 2014).

Both hSAMHD1 WT and a phospho-ablative mutant restrict HIV-1 infection in differentiated U937 cells, while phospho-mimetic mutants of hSAMHD1 lose the restriction of HIV-1 infection (Welbourn et al., 2013; White et al., 2013b). In our study, we found that WT hSAMHD1, WT and a phospho-ablative mutant (T634A) mSAMHD1 isoform 1, as well as WT mSAMHD1 isoform 2 lacking the T634 phosphorylation site, restricted HIV-1 infection in non-dividing cells, while a phospho-mimetic mutant of mSAMHD1 isoform 1 (T634D) lost restriction of HIV-1 infection in U937 cells. Overall, these results indicate that phosphorylation of mSAMHD1 isoform 1 at T634 also negatively regulates its restriction of HIV-1 infection.

We showed that phosphorylation of mSAMHD1 at T634 does not change its ability to reduce the dNTP pool in differentiated U937 cells, which is consistent with earlier reports that phosphorylation of hSAMHD1 does not alter its dNTPase activity in cells (Welbourn et al., 2013; White et al., 2013b). However, a recent study using in vitro assays showed impaired dNTPase activity of the phospho-mimetic mutation T592E compared to WT hSAMHD1 (Tang et al., 2015). This discrepancy might be due to different assays used in these studies. Moreover, the intracellular dNTP levels at one single time point were measured and used as an indicator of the dNTPase activity of SAMHD1 in cells (Welbourn et al., 2013; White et al., 2013b). It is also possible that, even with a decreased dNTPase activity, phospho-mimetic mutants of SAMHD1 may still be able to reduce the intracellular dNTP levels similarly compared to WT SAMHD1.

Non-dividing cells are refractory to MLV infection mainly because of limited nuclear import of MLV cDNA (Yamashita and Emerman, 2005). Therefore, we used a dividing mouse cell model to test SAMHD1's restriction of MLV infection. Our results suggest that MLV infection of dividing mouse cells can be inhibited by hSAMHD1 and mSAMHD1 at the stage of viral cDNA nuclear import, which is independent of T634 phosphorylation, but requires dNTPase function of SAMHD1. In contrast to MLV inhibition, we also observed that overexpression of WT hSAMHD1, mSAMHD1 isoform 1 or isoform 2 in dividing NIH3T3 cells did not affect HIV-1 infection. Given that SAMHD1 acts as a dNTPase in dividing cells, it is possible that overexpression of SAMHD1 can affect cell proliferation or cell cycle progression, thereby resulting in impeded MLV cDNA nuclear import and infection. Therefore, depletion of cellular dNTPs by SAMHD1 might have a restrictive effect on retroviral infection through other mechanisms in addition to blocking completion of viral reverse transcription.

Of note, conflicting results on the effect of mSAMHD1 on MLV infection have been reported. MLV infection is increased approximately 2-fold in a mouse macrophage cell line after mSAMHD1 knockdown compared to control cells (Zhang et al., 2014). In contrast, MLV infection was not affected in cells from SAMHD1-deficient mice relative to cells from WT mice (Behrendt et al., 2013; Rehwinkel et al., 2013). Differences in cell type and experimental approaches used could be confounding factors that lead to the inconsistent MLV restriction by mSAMHD1.

In summary, we identified six phosphosites in mSAMHD1 and demonstrated that CDK1 and CDK2 phosphorylate T634 of mSAMHD1 in dividing cells. T634 phosphorylation of mSAMHD1 regulate restriction of HIV-1 infection in non-dividing cells, but not MLV infection in dividing cells, suggesting different mechanisms of regulating retroviral restriction by hSAMHD1 and mSAMHD1.

Materials and Methods

Plasmids

The plasmids encoding hemagglutinin (HA)-hSAMHD1, HA-mSAMHD1 isoform 1 and empty vectors (Lahouassa et al., 2012) were kind gifts from Dr. Nathaniel Landau (New York University). Plasmids expressing HA-tagged mutant mSAMHD1 isoform 1 were generated using a Quickchange mutagenesis kit (Agilent Technologies) according to manufacturer's protocol. To generate mSAMHD1 T634A and T634D mutants, the following two primers were used, respectively: 5'-GCT CCA CTC ATA GCC CCT CTG AAA TGG -3' and 5'-GCT CCA CTC ATA GAC CCT CTG AAATGG -3'. The plasmids expressing HA-tagged WT or dominant negative (DN) mutant of CDK1 or CDK2 (van den Heuvel and Harlow, 1993) were purchased from Addgene.

Cell culture and generating stable cell lines expressing SAMHD1

Human embryonic kidney 293T (HEK293T) cells and a HIV-1 reporter cell line GHOST/X4/R5 have been described (Wu et al., 2002a; Wu et al., 2002b). Monocytic U937 cells lines were maintained as described (de Silva et al., 2013; Wang et al., 2007). U937 cells stably expressing WT hSAMHD1, WT mSAMHD1, or mutant mSAMHD1 (T634A or T634D) were generated by spinoculation of U937 cells with concentrated lentiviral vectors, and then cultured with 0.8 μg/mL puromycin containing media for selection as described (Hofmann et al., 2012; St Gelais et al., 2014). NIH3T3 cells were transduced with lentiviral vectors expressing hSAMHD1, mSAMHD1 WT or mutants for 2 hr, and then cultured with 2 μg/mL puromycin containing media (DMEM with 10% fetal bovine serum, and 1% penicillin and streptomycin) 48 h after the transduction. MEFs were maintained in DMEM with 10% fetal bovine serum, and 1% penicillin and streptomycin as described (Shembade et al., 2007).

Transfections of HEK293T cells

To produce lenti-viral vectors expressing hSAMHD1, mSAMHD1 WT, mSAMHD1 mutants or vector control, HEK293T cells were seeded at 3×10^5 cells/well in 6-well plates. After 24 hr, cells were transfected using a calcium phosphate method as described (St Gelais et al., 2014). To express WT or DN mutants of CDK1 or CDK2 in HEK293T cells, cells were seeded at 2×10^5 cells/well in 12-well plates. Plasmids encoding WT or DN mutant CDK1 or CDK2, or empty vectors (0.75 μg for each) were co-transfected with plenti-HA-mSAMHD1 vector (0.25 μg) as described (St Gelais et al., 2014).

Immunoblotting and antibodies

Cells were harvested at 24 h after transfection, and lysed with cell lysis buffer (Cell Signaling) containing protease inhibitor cocktail (Sigma-Aldrich). Cell lysates were

prepared for immunoblotting (Janas and Wu, 2009) and the blots were detected using antibodies specific against HA (Covance, Ha.11 clone 16B12), glyceraldehyde-3-phosphate dehydrogenase (GAPDH) (AbD serotec), CDK1 (Cell signaling, #9112), CDK2 (Santa Cruz, sc-163), SAMHD1 (Prosci, No.1224). Rabbit antibodies specific for phospho-SAMHD1 were generated by ProSci Inc. using phosphorylated hSAMHD1 peptide (Cribier et al., 2013): FTKPQDGDVIAPLI(Tp)PQKKE. The phospho-specific antibody was sequentially affinity-purified from the rabbit sera with a non-phospho-peptide conjugated column and a phospho-peptide conjugated column. Immunoblotting images were obtained and analyzed using Luminescent Image analyzer (LAS 4000) and Mutil-Gauge V3.0 software (Fuji Film) as described (St Gelais et al., 2012).

Mass Spectrometry

HEK293T cells were transfected to express HA-tagged mSAMHD1 and prepared for mass spectrometry as described (St Gelais et al., 2014). Peptides were analyzed at the Ohio State University Mass Spectrometry Core Facility using an LTQ-Orbitrap mass spectrometer. Tandem mass spectrometry samples were analyzed using Mascot (Matrix Science, version 2.4.1). Mascot was set up to search the SwissProt_ID_2013_02 database (selected for Mus musculus) assuming the digestion enzyme trypsin. Mascot was searched with a fragment ion mass tolerance of 0.80 Da and a parent ion tolerance of 20 PPM. Phosphorylation of serine, threonine and tyrosine were specified in Mascot as variable modifications. Analysis of identified peptides and phosphorylated residues was performed using Scaffold software with a minimum protein probability of 99.0% and minimum peptide probability of 95% (Proteome Software Inc.).

Treatment of cells with CDK1 and CDK2 inhibitors

HEK293T cells were pre-treated with specific inhibitors to CDK1 (Cribier et al., 2013) (CGP74513A, EMD Milliproe), CDK2 (Bramson et al., 2001) (Inhibitor II, Santa Cruz Biotech) at 1 μM, or dimethyl sulfoxide (DMSO) (Sigma-Aldrich) for 6 hr. Cells were transfected with plenti-HA-mSAHMD1 to express mSAMHD1 WT. The inhibitors were present during transfection, and at 12 h post-transfection fresh media with inhibitors were added. Cells were harvested at 24 h post-transfection, and processed for immunoblotting. NIH3T3 cells stably expressing mSAMHD1 isoform 1 were treated with specific inhibitors to CDK1 and CDK2 for 24 hours and then harvested for immunoblotting.

Knockdown of CDK1 and CDK2 in HEK293T cells by small interfering RNA (siRNA)

HEK293T cells were seeded in 12-well plates (3×10^5/well) at 24 h before transfection. Cells were transfected with 100 nM of SMARTpool ON-TARGET plus siRNA specific for CDK1 (L003224), CDK2 (L003236), or a scramble control (Dharmacon) using Trans-IT TKO (Mirus) according to manufacturer's protocol and two rounds of transfection were performed as described (St Gelais et al., 2014).

Virus stocks and infection assays

HIV-1 and MLV stocks were generated by transfecting HEK293T cells as described (de Silva et al., 2012). Virus stocks were harvested at 48 h post-transfection, and filtered

through 0.45 μM filters. To generate luciferase reporter HIV-1 pseudotyped with vesicular stomatitis virus G protein (HIV-luc/VSV-G), 10 μg pNL4-3-luc $E^{-}R^{+}$ and 4 μg pMD2-G (VSV-G) were used for transfection (Connor et al., 1995). To generate GFP reporter HIV-1 pseudotyped with VSV-G, 10 μg pHIV-CMV-GFP and 4 μg pMD2-G (VSV-G) were used for transfection (Mulky et al., 2008). To generate GFP reporter MLV (MLV-GFP/VSV-G), 10 μg pMIGR1, 5 μg pHIT60 and 4 μg pVSV-G were used (Mulky et al., 2008). HIV-1 stocks and MLV-GFP/VSV-G stocks were titrated with GHOST/X4/R5 cells (Wu et al., 2002b) and HEK293T cells, respectively.

For HIV-1 luc/VSV-G infection, U937 cells were treated with PMA and differentiated into non-dividing, macrophage-like cells (Laguette et al., 2011a). U937 cells were seeded in 96-well plates (1×10^5 per well) and treated with PMA (30 ng/mL) for 20 h. Cells were infected with HIV-1 at a multiplicity of infection (MOI) of 1 as described (Wang et al., 2009; Wu et al., 2002b). HIV-1 infection was determined by luciferase assays at 24 h post-infection (St Gelais et al., 2014). For infections with HIV-GFP/VSV-G and MLV-GFP/VSV-G, NIH3T3 stable cell lines were seeded in 24-well plates (6×10^4 cells/well). Cells were infected with MLV at a MOI of 1. The infection was determined by detecting GFP-positive cells with flow cytometry (GUAVA mini 2.0) at 48 h post-infection. The flow cytometry data were analyzed by FlowJo.

Quantitative PCR assays for MLV cDNA measurement

NIH3T3 stable cells were seeded in 24-well plates with 6×10^4 cells per well each cell line. MLV stocks were treated with 60 U/mL of TURBO DNase (Invitrogen, AM2238) for 30 minutes prior infection assay. Cells were treated with control media, AZT (5 μM) for 30 minutes prior MLV inoculation, and AZT was present for the duration of MLV infection. Cells were harvest at 24 h post infection for genomic DNA extraction using a DNeasy Blood & Tissue Kit (QIAGEN) followed with the manufactory's protocol.

The levels of late reverse transcription products and two one-long-terminal-repeat (2-LTR) circles of MLV in infected NIH3T3 cells were quantified by real-time quantitative PCR analysis using iQ™ SYBR® Green Supermix (BIO-RAD) followed protocol described in (Wu and Roth, 2014). Genomic DNA (50 ng) from MLV-infected NIH3T3 cells was used as the template for the detection of MLV late reverse transcription products and cellular GAPDH, and 250 ng of genomic DNA was used for the detection of MLV 2-LTR circles. GAPDH was used as an internal normalization control for each sample. The primers for genomic GAPDH detection are forward 5'-AGT ACT GCA GAG CCC CCG-3', and reverse 5'-GAT GAT GGA GGA CGT GAT GG -3' (Loffler et al., 2007). For the detection of MLV late reverse transcription products are: forward 5'-TTCTGTTCGCGCGCTTC -3', reverse 5'-TCC ACG ATT CGG ATG CAA AC-3'; for 2-LTR circle are: forward 5'-CGC CAG TCC TCC GAT AGA-3' and reverse 5'-CTGTTCCTAACCTTGATCTGAACT-3'. The data were analyzed using standard ΔΔCt method (Livak and Schmittgen, 2001).

Intracellular dNTP measurement

For dNTP analysis and quantification, cells were harvested and lysed in iced cold 65% methanol, and vigorously vortexed for 2 minutes. Extracts were incubated at 95°C for 3

minutes. Supernatants were collected and dried in a speed vacuum. Samples were processed for the single nucleotide incorporation assay as described (Diamond et al., 2004).

Statistical analysis

The data were analyzed by one-way ANOVA followed with Dunnett's test, or by t-test in Graphpad 5.0. The statistical significance was defined as $P < 0.05$.

Acknowledgements

We thank Nathaniel Landau (New York University) for SAMHD1-expressing constructs, Vineet KewalRamani (National Cancer Institute) for U937 cell line and MLV vector. AZT was obtained through the AIDS Research and Reference Reagent Program, Division of AIDS, NIAID, NIH. This work was supported by an NIH grant AI104483 to LW. LW is also supported in part by the Public Health Preparedness for Infectious Diseases Program of The Ohio State University and by NIH grants (CA181997 and AI120209). FW is supported by the C. Glenn Barber Fund from the Ohio State University. JSY is supported by NIH grants AI095348 and AI114826. BK is supported by NIH grants AI049781 and GM104198. We thank Jocelyn Hach and Heather Hoy for excellent technical assistance and the members of the Wu laboratory for helpful discussions.

References

Baldauf HM, Pan X, Erikson E, Schmidt S, Daddacha W, Burggraf M, Schenkova K, Ambiel I, Wabnitz G, Gramberg T, Panitz S, Flory E, Landau NR, Sertel S, Rutsch F, Lasitschka F, Kim B, Konig R, Fackler OT, Keppler OT. SAMHD1 restricts HIV-1 infection in resting CD4(+) T cells. Nat Med. 2012; 18:1682–1687. [PubMed: 22972397]

Behrendt R, Schumann T, Gerbaulet A, Nguyen LA, Schubert N, Alexopoulou D, Berka U, Lienenklaus S, Peschke K, Gibbert K, Wittmann S, Lindemann D, Weiss S, Dahl A, Naumann R, Dittmer U, Kim B, Mueller W, Gramberg T, Roers A. Mouse SAMHD1 has antiretroviral activity and suppresses a spontaneous cell-intrinsic antiviral response. Cell Rep. 2013; 4:689–696. [PubMed: 23972988]

Bramson HN, Corona J, Davis ST, Dickerson SH, Edelstein M, Frye SV, Gampe RT, Harris PA, Hassell A, Holmes WD, Hunter RN, Lackey KE, Lovejoy B, Luzzio MJ, Montana V, Rocque WJ, Rusnak D, Shewchuk L, Veal JM, Walker DH, Kuyper LF. Oxindole-based inhibitors of cyclin-dependent kinase 2 (CDK2): Design, synthesis, enzymatic activities, and X-ray crystallographic analysis. Journal of Medicinal Chemistry. 2001; 44:4339–4358. [PubMed: 11728181]

Connor RI, Chen BK, Choe S, Landau NR. Vpr is required for efficient replication of human immunodeficiency virus type-1 in mononuclear phagocytes. Virology. 1995; 206:935–944. [PubMed: 7531918]

Cribier A, Descours B, Valadao AL, Laguette N, Benkirane M. Phosphorylation of SAMHD1 by Cyclin A2/CDK1 Regulates Its Restriction Activity toward HIV-1. Cell Rep. 2013; 3:1036–1043. [PubMed: 23602554]

de Silva S, Hoy H, Hake TS, Wong HK, Porcu P, Wu L. Promoter Methylation Regulates SAMHD1 Gene Expression in Human CD4(+) T Cells. J Biol Chem. 2013; 288:9284–9292. [PubMed: 23426363]

de Silva S, Planelles V, Wu L. Differential effects of Vpr on single-cycle and spreading HIV-1 infections in CD4+ T-cells and dendritic cells. PLoS One. 2012; 7:e35385. [PubMed: 22570689]

Diamond TL, Roshal M, Jamburuthugoda VK, Reynolds HM, Merriam AR, Lee KY, Balakrishnan M, Bambara RA, Planelles V, Dewhurst S, Kim B. Macrophage tropism of HIV-1 depends on efficient cellular dNTP utilization by reverse transcriptase. J Biol Chem. 2004; 279:51545–51553. [PubMed: 15452123]

Goldstone DC, Ennis-Adeniran V, Hedden JJ, Groom HC, Rice GI, Christodoulou E, Walker PA, Kelly G, Haire LF, Yap MW, de Carvalho LP, Stoye JP, Crow YJ, Taylor IA, Webb M. HIV-1 restriction factor SAMHD1 is a deoxynucleoside triphosphate triphosphohydrolase. Nature. 2011; 480:379–382. [PubMed: 22056990]

Gramberg T, Kahle T, Bloch N, Wittmann S, Mullers E, Daddacha W, Hofmann H, Kim B, Lindemann D, Landau NR. Restriction of diverse retroviruses by SAMHD1. Retrovirology. 2013; 10:26. [PubMed: 23497255]

Hofmann H, Logue EC, Bloch N, Daddacha W, Polsky SB, Schultz ML, Kim B, Landau NR. The Vpx lentiviral accessory protein targets SAMHD1 for degradation in the nucleus. J Virol. 2012; 86:12552–12560. [PubMed: 22973040]

Hrecka K, Hao C, Gierszewska M, Swanson SK, Kesik-Brodacka M, Srivastava S, Florens L, Washburn MP, Skowronski J. Vpx relieves inhibition of HIV-1 infection of macrophages mediated by the SAMHD1 protein. Nature. 2011; 474:658–661. [PubMed: 21720370]

Janas AM, Wu L. HIV-1 interactions with cells: from viral binding to cell-cell transmission. Curr Protoc Cell Biol. 2009:25. Chapter 26, Unit 26.

Kim ET, White TE, Brandariz-Nunez A, Diaz-Griffero F, Weitzman MD. SAMHD1 Restricts Herpes Simplex Virus 1 in Macrophages by Limiting DNA Replication. J Virol. 2013; 87:12949–12956. [PubMed: 24067963]

Laguette N, Sobhian B, Casartelli N, Ringeard M, Chable-Bessia C, Segeral E, Yatim A, Emiliani S, Schwartz O, Benkirane M. SAMHD1 is the dendritic- and myeloid-cell-specific HIV-1 restriction factor counteracted by Vpx. Nature. 2011a; 474:654–657. [PubMed: 21613998]

Laguette N, Sobhian B, Casartelli N, Ringeard M, Chable-Bessia C, Segeral E, Yatim A, Emiliani S, Schwartz O, Benkirane M. SAMHD1 is the dendritic- and myeloid-cell-specific HIV-1 restriction factor counteracted by Vpx. Nature. 2011b; 474:654–657. [PubMed: 21613998]

Lahouassa H, Daddacha W, Hofmann H, Ayinde D, Logue EC, Dragin L, Bloch N, Maudet C, Bertrand M, Gramberg T, Pancino G, Priet S, Canard B, Laguette N, Benkirane M, Transy C, Landau NR, Kim B, Margottin-Goguet F. SAMHD1 restricts the replication of human immunodeficiency virus type 1 by depleting the intracellular pool of deoxynucleoside triphosphates. Nat Immunol. 2012; 13:223–228. [PubMed: 22327569]

Livak KJ, Schmittgen TD. Analysis of relative gene expression data using real-time quantitative PCR and the 2(-Delta Delta C(T)) Method. Methods. 2001; 25:402–408. [PubMed: 11846609]

Loffler KA, Biondi CA, Gartside M, Waring P, Stark M, Serewko-Auret MM, Muller HK, Hayward NK, Kay GF. Broad tumor spectrum in a mouse model of multiple endocrine neoplasia type 1. Int J Cancer. 2007; 120:259–267. [PubMed: 17044021]

Malumbres M, Barbacid M. Mammalian cyclin-dependent kinases. Trends Biochem Sci. 2005; 30:630–641. [PubMed: 16236519]

Mulky A, Cohen TV, Kozlov SV, Korbei B, Foisner R, Stewart CL, KewalRamani VN. The LEM domain proteins emerin and LAP2alpha are dispensable for human immunodeficiency virus type 1 and murine leukemia virus infections. J Virol. 2008; 82:5860–5868. [PubMed: 18400857]

Pauls E, Ruiz A, Badia R, Permanyer M, Gubern A, Riveira-Munoz E, Torres-Torronteras J, Alvarez M, Mothe B, Brander C, Crespo M, Menendez-Arias L, Clotet B, Keppler OT, Marti R, Posas F, Ballana E, Este JA. Cell Cycle Control and HIV-1 Susceptibility Are Linked by CDK6-Dependent CDK2 Phosphorylation of SAMHD1 in Myeloid and Lymphoid Cells. J Immunol. 2014; 193:1988–1997. [PubMed: 25015816]

Powell RD, Holland PJ, Hollis T, Perrino FW. Aicardi-Goutieres syndrome gene and HIV-1 restriction factor SAMHD1 is a dGTP-regulated deoxynucleotide triphosphohydrolase. J Biol Chem. 2011; 286:43596–43600. [PubMed: 22069334]

Rehwinkel J, Maelfait J, Bridgeman A, Rigby R, Hayward B, Liberatore RA, Bieniasz PD, Towers GJ, Moita LF, Crow YJ, Bonthron DT, Reis e Sousa C. SAMHD1-dependent retroviral control and escape in mice. EMBO J. 2013; 32:2454–2462. [PubMed: 23872947]

Ryoo J, Choi J, Oh C, Kim S, Seo M, Kim SY, Seo D, Kim J, White TE, Brandariz-Nunez A, Diaz-Griffero F, Yun CH, Hollenbaugh JA, Kim B, Baek D, Ahn K. The ribonuclease activity of SAMHD1 is required for HIV-1 restriction. Nat Med. 2014; 20:936–941. [PubMed: 25038827]

Shembade N, Harhaj NS, Yamamoto M, Akira S, Harhaj EW. The human T-cell leukemia virus type 1 Tax oncoprotein requires the ubiquitin-conjugating enzyme Ubc13 for NF-kappaB activation. Journal of virology. 2007; 81:13735–13742. [PubMed: 17942533]

St Gelais C, de Silva S, Amie SM, Coleman CM, Hoy H, Hollenbaugh JA, Kim B, Wu L. SAMHD1 restricts HIV-1 infection in dendritic cells (DCs) by dNTP depletion, but its expression in DCs and

primary CD4+ T-lymphocytes cannot be upregulated by interferons. Retrovirology. 2012; 9:105. [PubMed: 23231760]

St Gelais C, de Silva S, Hach JC, White TE, Diaz-Griffero F, Yount JS, Wu L. Identification of Cellular Proteins Interacting with the Retroviral Restriction Factor SAMHD1. J Virol. 2014; 88:5834–5844. [PubMed: 24623419]

Sweet SM, Bailey CM, Cunningham DL, Heath JK, Cooper HJ. Large scale localization of protein phosphorylation by use of electron capture dissociation mass spectrometry. Mol Cell Proteomics. 2009; 8:904–912. [PubMed: 19131326]

Tang C, Ji X, Wu L, Xiong Y. Impaired dNTPase activity of SAMHD1 by phosphomimetic mutation of T592. J Biol Chem. 20152015 ePub on Aug 20.

van den Heuvel S, Harlow E. Distinct roles for cyclin-dependent kinases in cell cycle control. Science. 1993; 262:2050–2054. [PubMed: 8266103]

Villen J, Beausoleil SA, Gerber SA, Gygi SP. Large-scale phosphorylation analysis of mouse liver. Proc Natl Acad Sci U S A. 2007; 104:1488–1493. [PubMed: 17242355]

Wang JH, Janas AM, Olson WJ, KewalRamani VN, Wu L. CD4 coexpression regulates DC-SIGN-mediated transmission of human immunodeficiency virus type 1. J Virol. 2007; 81:2497–2507. [PubMed: 17151103]

Wang JH, Kwas C, Wu L. Intercellular adhesion molecule 1 (ICAM-1), but not ICAM-2 and -3, is important for dendritic cell-mediated human immunodeficiency virus type 1 transmission. J Virol. 2009; 83:4195–4204. [PubMed: 19211748]

Welbourn S, Dutta SM, Semmes OJ, Strebel K. Restriction of virus infection but not catalytic dNTPase activity is regulated by phosphorylation of SAMHD1. J Virol. 2013; 87:11516–11524. [PubMed: 23966382]

White TE, Brandariz-Nunez A, Valle-Casuso JC, Amie S, Nguyen L, Kim B, Brojatsch J, Diaz-Griffero F. Contribution of SAM and HD domains to retroviral restriction mediated by human SAMHD1. Virology. 2013a; 436:81–90. [PubMed: 23158101]

White TE, Brandariz-Nunez A, Valle-Casuso JC, Amie S, Nguyen LA, Kim B, Tuzova M, Diaz-Griffero F. The retroviral restriction ability of SAMHD1, but not its deoxynucleotide triphosphohydrolase activity, is regulated by phosphorylation. Cell Host Microbe. 2013b; 13:441–451. [PubMed: 23601106]

Wu DT, Roth MJ. MLV based viral-like-particles for delivery of toxic proteins and nuclear transcription factors. Biomaterials. 2014; 35:8416–8426. [PubMed: 24997480]

Wu L. Cellular and Biochemical Mechanisms of the Retroviral Restriction Factor SAMHD1. ISRN Biochem. 2013; 2013:11.

Wu L, Bashirova AA, Martin TD, Villamide L, Mehlhop E, Chertov AO, Unutmaz D, Pope M, Carrington M, KewalRamani VN. Rhesus macaque dendritic cells efficiently transmit primate lentiviruses independently of DC-SIGN. Proc Natl Acad Sci U S A. 2002a; 99:1568–1573. [PubMed: 11818554]

Wu L, Martin TD, Vazeux R, Unutmaz D, KewalRamani VN. Functional Evaluation of DC-SIGN Monoclonal Antibodies Reveals DC-SIGN Interactions with ICAM-3 Do Not Promote Human Immunodeficiency Virus Type 1 Transmission. J. Virol. 2002b; 76:5905–5914. [PubMed: 12021323]

Yamashita M, Emerman M. The cell cycle independence of HIV infections is not determined by known karyophilic viral elements. PLoS Pathog. 2005; 1:e18. [PubMed: 16292356]

Yang S, Shan T, Zhou Y, Jiang Y, Tong W, Liu F, Wen F, Zhang Q, Tong G. Molecular cloning and characterizations of porcine SAMHD1 and its roles in replication of highly pathogenic porcine reproductive and respiratory syndrome virus. Dev Comp Immunol. 2014; 47:234–246. [PubMed: 25106914]

Zanivan S, Gnad F, Wickstrom SA, Geiger T, Macek B, Cox J, Fassler R, Mann M. Solid tumor proteome and phosphoproteome analysis by high resolution mass spectrometry. J Proteome Res. 2008; 7:5314–5326. [PubMed: 19367708]

Zhang R, Bloch N, Nguyen LA, Kim B, Landau NR. SAMHD1 restricts HIV-1 replication and regulates interferon production in mouse myeloid cells. PLoS One. 2014; 9:e89558. [PubMed: 24586870]

Research Highlights

- Mouse SAMHD1 (mSAMHD1) restricts HIV-1 infection, but its regulation is unknown
- Six phospho-sites of mSAMHD1 were identified by mass spectrometry
- T634 of mSAMHD1 is phosphorylated by CDK1 and CDK2
- mSAMHD1 restricts MLV infection in dividing cells
- T634 phosphorylation of mSAMHD1 negatively regulates HIV-1, but not MLV restriction

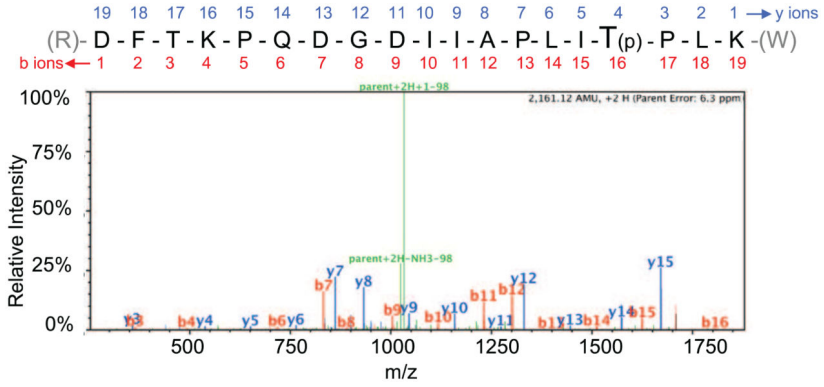

Fig. 1.

Residue T634 in the mSAMHD1 protein sequence is a phosphosite as identified by tandem mass spectrometry. Position T634 was identified as a phosphosite by MS/MS analysis. An example MS/MS spectrum is shown for the indicated tryptic peptide of mSAMHD1 (residues 619 to 637) that identified the T634 phosphorylation site, which is highlighted in the sequence and denoted by a “(p)”. Assigned b ions are shown in red, and y ions are shown in blue. Green peaks represent loss of a 98 Da fragment that corresponds to loss of a phosphate group as indicated.

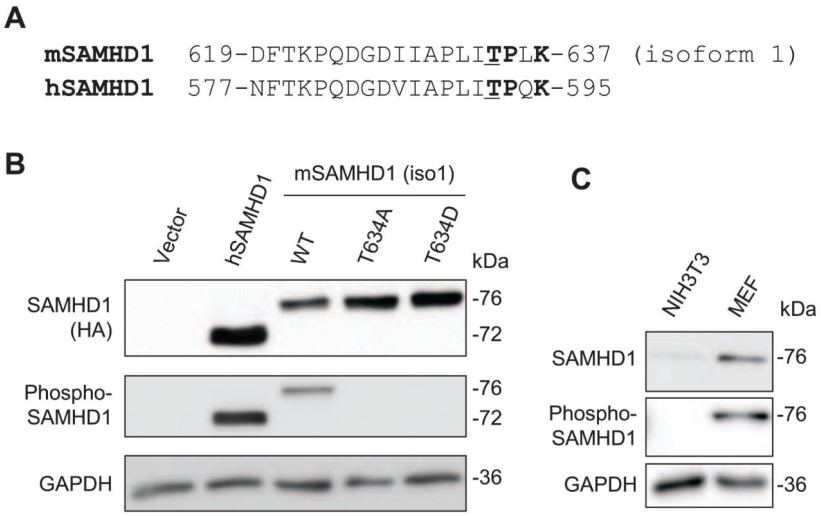

Fig. 2.

Confirmation of the phosphorylation of mSAMHD1 at position T634 using a phospho-specific antibody. (A) Partial protein sequence alignment of mSAMHD1 isoform 1 and human (hSAMHD1) depicting conserved phosphosites at residue positions T634 and T592 in mSAMHD1 and hSAMHD1 sequences, respectively. The phosphorylated residue threonine (T) is underlined and the residues encompassing a consensus sequence (TPXK) for CDK interaction are highlighted in bold. (B) HEK293T cells were transiently transfected to overexpress hSAMHD1, mSAMHD1 wild-type (WT), phospho-ablative mutant (T634A) or phospho-mimetic mutant (T634D). Immunoblotting was performed on cell lysates to confirm position T634 of mSAMHD1 is a phosphosite. Total SAMHD1 protein levels were probed using an anti-HA antibody (top panel). (C) Endogenous mSAMHD1 in mouse embryonic fibroblasts (MEFs) is phosphorylated at T634. The total SAMHD1 was probed with a specific SAMHD1 antibody. (B) and (C) The phospho-SAMHD1 levels were detected using a phospho-specific SAMHD1 antibody (middle panel). GAPDH was used as a loading control. A representative immunoblot result from three independent experiments is shown.

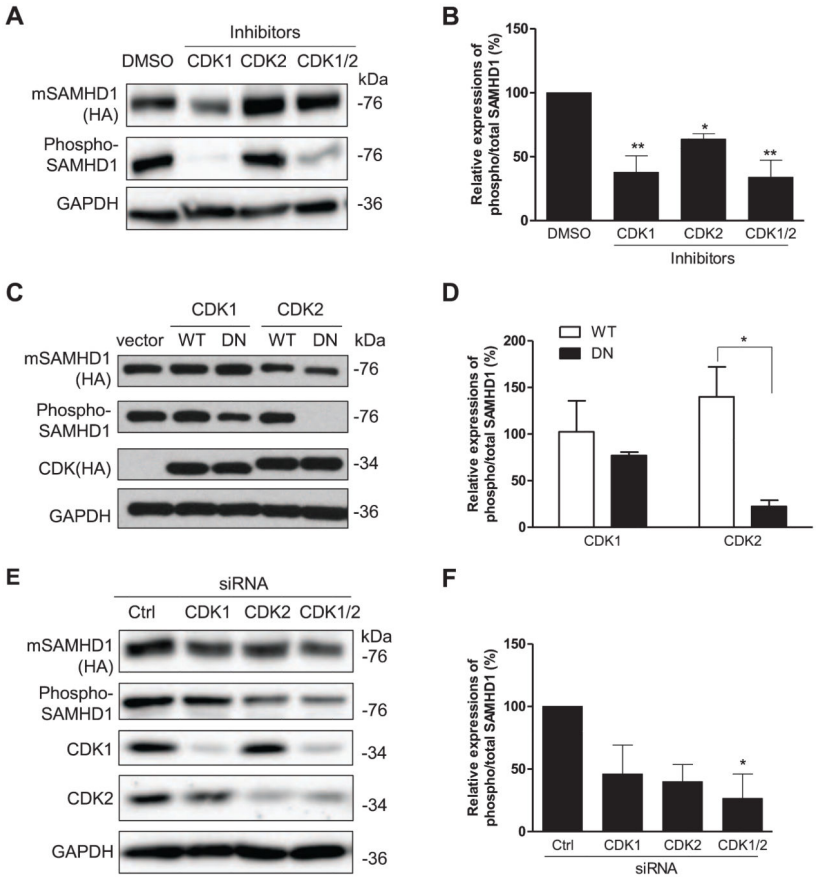

Fig. 3.

CDK1 and CDK2 contribute to T634 phosphorylation of mSAMHD1 in HEK293T cells. (A) Cells were pre-treated with DMSO or inhibitors specific to CDK1 or CDK2 at 1 μM for 6 h and transiently transfected to overexpress mSAMHD1. The effect of each inhibitor on the phosphorylation of mSAMHD1 at T634 was assessed at 24 h post-transfection by immunoblotting. (B) An average of three independent experiments described in (A). (C) mSAMHD1 was overexpressed together with wild-type (WT) or dominant negative (DN) mutants of CDK1 or CDK2. Empty vector was used as a negative control. At 24 h post-transfection, cells were harvested for immunoblotting to determine total SAMHD1, phosphorylated SAMHD1 and CDK expression levels. Total mSAMHD1 and CDK1/2 protein levels were detected using an HA-specific antibody and phosphorylation of T634 was detected using a phospho-specific SAMHD1 antibody. (D) An average of three independent experiments described in (C). (E) Individual and combined siRNA-mediated knockdown of endogenous CDK1 and CDK2 were performed in the presence of ectopically expressed mSAMHD1 using a two-round transfection protocol. Cells were harvested 24 h following the second round of siRNA transfection and cell lysates were subjected to immunoblotting to determine the effect of CDK1/2 knockdown on the phosphorylation of mSAMHD1 at T634. The efficiency of siRNA-mediated knockdown of CDK1 and CDK2 was determined by probing with their respective antibodies. (F) An average of three independent experiments described in (E). In (A, C and E), total SAMHD1 levels were detected using an HA-specific antibody. The levels of phospho-SAMHD1 were detected

using a phospho-SAMHD1 specific antibody. GAPDH was used as a loading control. In (B, D and F), the protein levels were quantified based on the band densities. The levels of total mSAMHD1 and phospho-SAMHD1 were normalized to GAPDH respectively, and then the ratio of phospho/total mSAMHD1 was calculated and the ratio of the vector group was set as 1. Results are shown as mean ± SD (n=3). The data was analyzed by T-test or one-way ANOVA with Dunnett's test (*, $P < 0.05$, **, $P < 0.01$).

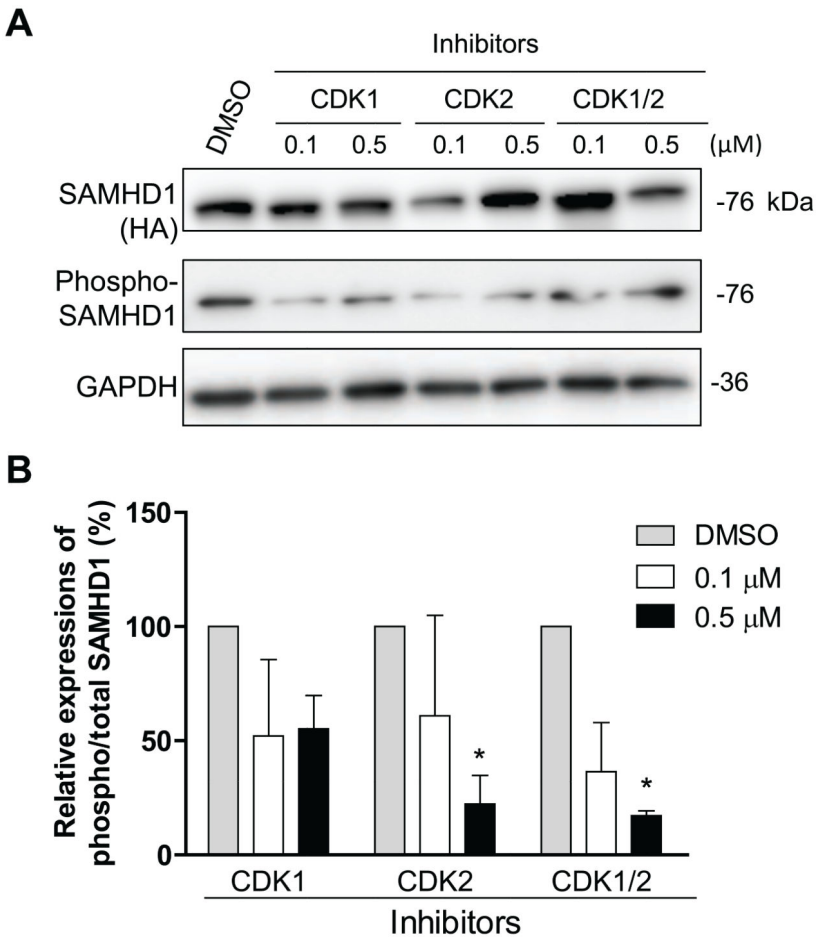

Fig. 4.

Endogenous CDK1 and CDK2 phosphorylate mSAMHD1 at T634 in mouse fibroblast cells. (A) NIH3T3 cells stably expressing mSAMHD1 were treated with inhibitors specific to CDK1 or CDK2 at the indicated concentrations. The effects of each inhibitor on the phosphorylation of mSAMHD1 at T634 were assessed at 24 h post-transfection by immunoblotting with a phospho-specific antibody. (B) An average of three independent experiments. The protein levels were quantified based on the band densities. The levels of total mSAMHD1 and phospho-SAMHD1 were normalized to GAPDH, and then the ratio of phospho/total mSAMHD1 was calculated and the ratio of the vector group was set as 100%. Results are shown as mean ± SD (n=3). The data was analyzed by one-way ANOVA with Dunnett's test (*, $P < 0.05$).

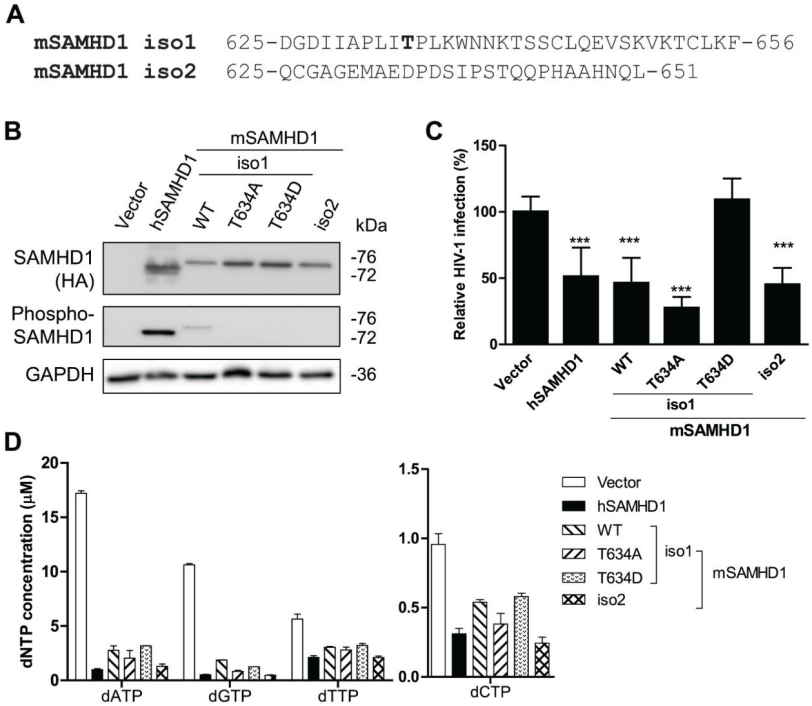

Fig. 5.

The effect of T634 phosphorylation of mSAMHD1 on its restriction of HIV-1 infection in PMA-differentiated U937 cells. (A) The C-terminus alignment of mSAMHD1 isoform 1 (iso1) and isoform 2 (iso2) proteins illustrating the T634 region is lacking in the iso2 protein. (B) The expression levels of total and phosphorylated SAMHD1 (WT and mutants) in U937 stable cell lines were determined by immunoblotting with an anti-HA antibody and specific phospho-SAMHD1 antibody, respectively. GAPDH was used as a loading control. (C) U937 cells expressing hSAMHD1 WT, mSAMHD1 WT, phospho-ablative mutant (T634A), phospho-mimetic mutant (T634D) or an empty vector were infected with a single-cycle HIV-1 luc/VSV-G at a multiplicity of infection (MOI=1). At 24 h post-infection, cells were harvested for luciferase assay to measure HIV-1 infection. An average of three independent infection experiments is presented (n=12). The infection level in the vector control group was set as 100% for normalization. (D) The levels of intracellular dNTPs were significantly decreased by hSAMHD1, mSAMHD1 WT or mutants compared to the vector control ($P < 0.0001$). The results are shown as mean ± SD (n =2). The dNTP concentrations were calculated based on the cell volume of human primary macrophages (2,660 μm^3). For (C-D), statistical analysis was performed by one-way ANOVA and Dunnett's test (***, $P < 0.0001$).

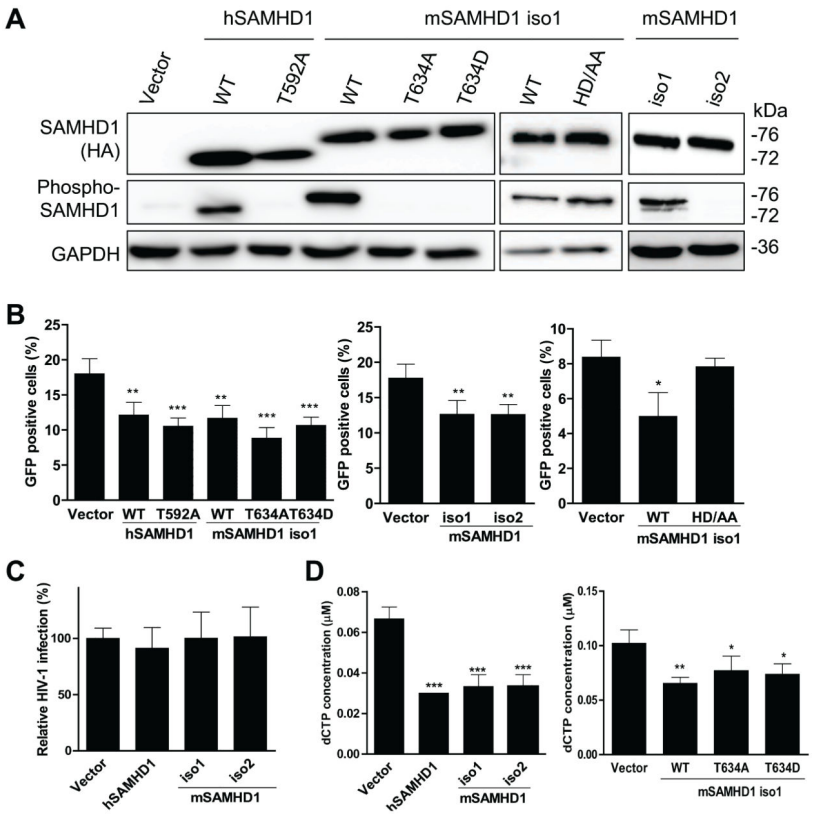

Fig. 6.

MLV infection in dividing NIH3T3 cells is reduced by mSAMHD1 independently of its T634 phosphorylation. (A) Overexpression of HA-tagged mSAMHD1 isoform 1 (iso1) and isoform 2 (iso2) proteins and iso1 mutants in NIH3T3 stable cells lines was confirmed by immunoblotting using anti-HA antibody. Vector-transduced cells were used as a negative control. Phosphorylation status of hSAMHD1 (T592) and mSAMHD1 (T634) was assessed using a phospho-specific antibody. GAPDH was used as a loading control. (B) Overexpression of SAMHD1 WT or iso1 phospho-mutants, but not the dNTPase-defective mSAMHD1 iso1 mutant H238A/D239A (HD/AA), in NIH3T3 cells modestly reduces MLV infection. (C) HIV-1 infection is not restricted by WT hSAMHD1, WT mSAMHD1 iso1, or WT mSAMHD1 iso2 in NIH3T3 cells. NIH3T3 cells were infected with a single-cycle MLV-GFP/VSV-G reporter virus (B) or an HIV-1-GFP/VSV-G reporter virus (C) (MOI=1). At 48 h post-infection, cells were harvested to determine the percentage of GFP-positive cells by flow cytometry. (D) Intracellular dCTP levels were reduced in NIH3T3 cells expressing WT hSAMHD1, WT mSAMHD1 or phospho-mutants of mSAMHD1. The concentrations calculated based on the average cell size of NIH3T3 (diameter is 18 μm) and the spherical cell assumption. The data were analyzed by one-way ANOVA and Dunnett's test (*, $P < 0.05$, **, $P < 0.01$, ***, $P < 0.0001$).

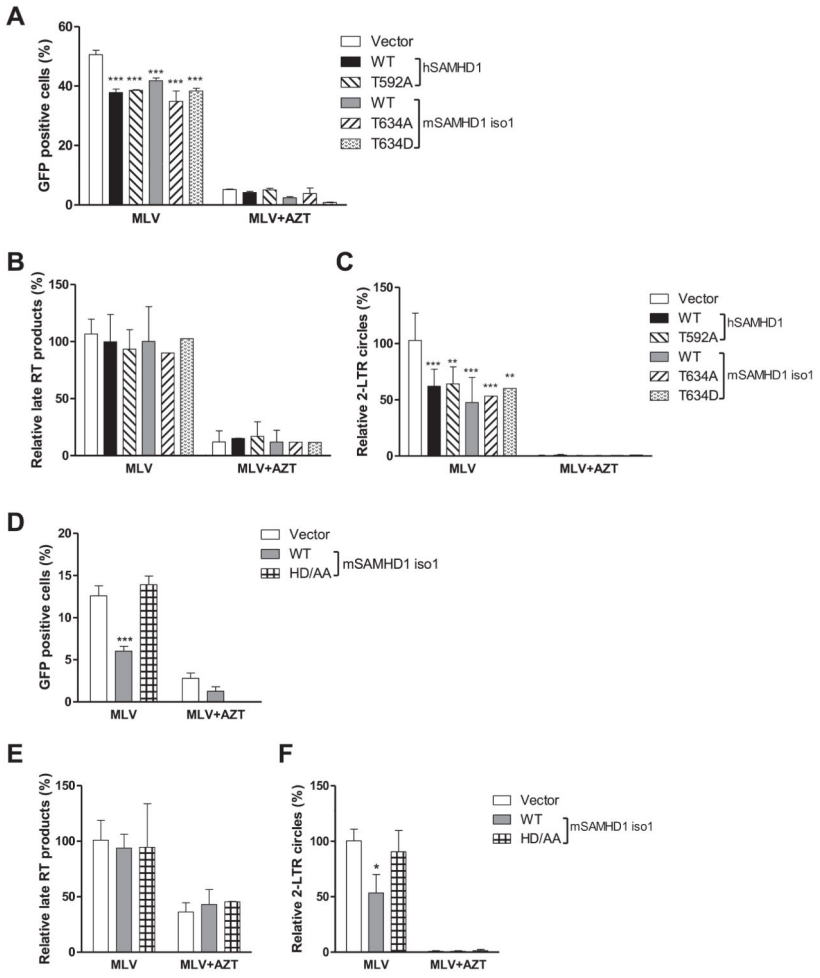

Fig. 7.

MLV infection in dividing NIH3T3 cells is inhibited by mSAMHD1 at the viral cDNA nuclear import stage but not the late RT step. (A and D) MLV infection in cells expressing WT or mutant SAMHD1 was reduced by AZT treatment (5 μM). (B and E) The levels of late reverse transcription (RT) products in MLV infected cells were not affected by overexpression of SAMHD1 WT or mutants in NIH3T3 cells. (C and F) The levels of 2-LTR circles were reduced by overexpression of SAMHD1 WT or phospho-mutants in NIH3T3 cells, the AZT treatment, but not overexpression of the HD/AA mutant of mSAMHD1 isoform 1 (iso1). (A-F) Cells were infected with MLV-GFP/VSV-G (MOI=1) in the presence of control media or AZT (5 μM). Cells were harvested at 24 h post-infection and used for genomic DNA extraction. The levels of MLV late RT products (B and E) and of 2-LTR circles (C and F) were measured using real-time PCR. An average of three independent experiments was presented. After normalization to GAPDH, the levels of late reverse transcription products or 2-LTR circles in MLV-infected vector control cells were set as 100%. The data were analyzed by one-way ANOVA and Dunnett's test (*, $P < 0.05$, **, $P < 0.01$, ***, $P < 0.0001$).

Table 1

Mapping mouse SAMHD1 phosphorylation sites by mass spectrometry

	% Residues Mapped [a]	Phosphorylation sites [b]
Serines (S)	72% (26/36)	S55, S140
Threonines (T)	83% (20/24)	T52, T56, T310, T634
Total Residues	72% (476/658)	Indicated above

[a] The percentages of covered residues over total residue in MS/MS data.

[b] Residue positions of phosphorylated serines (S) and threonines (T) were identified by MS/MS analysis.